ISSN (Print) 1226-1750
ISSN (Online) 2233-6656
Journal of Magnetics 28(2), 91-101 (2023) https://doi.org/10.4283/JMAG.2023.28.2.91

Design Analysis of Amended PIFA with Ferrite Sheet Attachment for SAR Reduction in Human Head

P. Ashok Kumar[1]* and Ch. R. Phani Kumar[2]

[1]*Research Scholar, Department of ECE, GITAM Deemed to be University, Visakhapatnam, Andhra Pradesh, India*
[2]*Assistant Professor, Department of ECE, GITAM Deemed to be University, Visakhapatnam, Andhra Pradesh, India*

(Received 13 June 2022, Received in final form 3 February 2023, Accepted 6 February 2023)

The public's growing awareness of the negative impacts of high-volume temperature fluctuations has led to a marked rise in the Specific Absorption Rate (SAR). In existing techniques, the SAR value is high and more expensive. To overcome this issue, an Amended Planar Inverted F-antenna (PIFA) with Ferrite Sheet Attachment for SAR Reduction in Human Head has been introduced to reduce SAR value. The antenna receives power from the grounded end and Simulated Magnetic Rods (SMR) are utilized in the antenna to lower SAR values. The PIFA and SMR face major difficulties due to their low reliability and bandwidth. Hence, Radiating Blotch is implemented within the antenna to increase bandwidth and dependability. The SAR reduction is increased and various parameters are produced when the header model is simulated using ANSYS HFSS. Overall, the performance with and without a ferrite sheet comparing the analysis for SAR reduction with various parameters.

Keywords : Planar Inverted F-Antenna (PIFA), simulated magnetic rod (SMR), Specific absorption rate (SAR), ferrite sheet attachment

1. Introduction

For immunology-telemetry applications, implantable antennas have recently become critical and one of the main parameters to be taken good care of for an implantable Specific Absorption Rate (SAR) antenna. In the region near the ground, SAR is dependent on the application of electric fields. Because as the general public is becoming aware of the adverse effects of exposure to high-volume microwave ovens, specific absorption rate (SAR) has gained growing attention [1]. This could create hot spots in the human body which could contribute to tissue destruction. A low SAR system would be ideal in applications where antennas have to be positioned in the vicinity of the human body (portable or body-worn computers, Body Area Networks, pagers, etc.). Two separate polymeric ferrite sheets (PFS) were tested for SAR reduction at 2.4 GHz in the work mentioned in the letter [2]. Consequently, it can be supposed that the new distribution's uniformity contributes to a lowering of the SAR value. The ferrite layer will usually stand used towards decreased breaks aimed at an antenna inside the current distribution [3]. Ferrites are the most significant category of ferromagnetic materials. Since the permeability of ferrites is low, when electromagnetic frequencies are applied, less current is induced in the material. The current density over the antenna was suppressed by the ferrite layer, resulting in the corresponding SAR surface being reduced. A ferrite sheet can be optimized to achieve the maximum reduction in the SAR values using the information mentioned above about the SAR rapidly deteriorating.

A successful solution to reducing the SAR in the human head is to use a planar antenna integrated on the back (away from the source) of a mobile telephone. But, especially in achieving the necessary frequency bandwidth and radiation productivity, it brings additional design challenges. Another option is the use of a longitudinal or reflective antenna [4, 5]. The availability of signals obtained from all directions to the portable telephone is sacrificed by such an antenna arrangement. The authors suggested adding a sheet of ferrite to the front (near the head) of the cell phone. Due to the reduction of surface currents on the front side of the portable phone, the

*Corresponding author: Tel:
Fax: , e-mail: ashok.pentaece@gmail.com

process of SAR reduction by ferrite sheet attachment was explained [6]. Current media issues are the safety of mobile phones and the application of relevant advertisement standards, and regulatory authorities are motivated to ensure that compliance monitoring is effective. Specify protocols and methods for measuring the peak temporal-average specific absorption rate (SAR) induced by handheld radio transceivers (cell phones) within a simplified user-head configuration. For eg, in a SAR 1 gm averaging mass, the SAR limit condensed at 1.6 W/kg while that was changed to 2 W/kg in a 10 gm averaged mass [7]. Compared to the cap simplified in the Recommendations of the International Commission on Non-Ionizing Radiation Safety (ICNIRP), this new SAR cap has been simplified. The routine SAR evaluation of the telephone model before system authorization or use since 1997 is required by the Federal Communication Commission (FCC) [8]. Here remains actually towards diminish the exertion in the phone model's design stage to reduce the spatial peak SAR, since the risk of a spatial peak SAR exceeding the prescribed exposure limit cannot be completely excluded [9]. Several published papers investigated the cellular handset's interaction with the human head; The person head of the antenna on the antennas of the phone, including amplitude, gain, and quality of feed points; secondly, the effect of radiation EM antenna on the head of the consumer due to the energy taken in by the SAR prediction in the tissue of the head.

In general, the troubles in the reduction of SAR include correct cellular telephone representation; anatomic head image; phone and head alignment, as well as a suitable ferrite sheet or other material design. Human susceptibility to electromagnetic (EM) radiation, together with the health effects associated with it, is a matter of public concern and scientific research is ongoing [10, 11]. A variety of studies have been carried out on this topic and the consequences of mobile users are often discussed. However, computers and terminals in other frequency bands have gained significant interest in the last 15 years. A sheet of ferrite was introduced as an attachment of protection between the antenna and the human head [12]. A reduction of more than 13 percent was achieved over a 1 gm average for the spatial peak SAR. A study on the effects of ferrite sheets on SAR reduction was proposed and the protecting position played an important role to reduce performance.

Besides SAR in the human head, the use of a planar antenna, which is integral on the rear of a phone model, is an appropriate method, but it does have additional design problems, particularly in terms of achieving the necessary frequency bandwidth and radiation efficiency [13, 14]. The use of a directional or reflective antenna is another method. Such an antenna design sacrifices the efficiency of the signals sent out from all directions to the telephone model. The SAR reduction method by ferrite sheet attachment is suppressed thanks to surface interactions at the front of the specific phone. There were many issues with the existing design, such as high operating frequency, high radiation rate, durability, and high SAR value. We present the ferrite sheet with a Planar Inverted F-antenna for SAR reduction in this novel configuration.

2. Literature Survey

Lwin *et al.* [15] study of the current world have shown electromagnetic waves traveling across the human body from different forms of transmitting antennas, such as in phones. The human body absorbs the EM wave and some unnecessary impacts occur in the tissues. The Specific Absorption Rate (SAR) is a useful parameter to quantify these impacts. In this review, the temperature variations in the human body are measured in a tissue-based SAR analysis and are known as thermal effects. The FDTD approach and the bio-heat equation are primarily used to calculate the effect. The FDTD approach is used for the calculation. In the two-dimensional computer model FDTD, electrical field propagation in two polarizations is studied: the electrical wave, the transverse electrical wave, and the magnetic magnet (TM) wave. The source of the electric field is held close to the human head that is constructed as organized layers.

Ahmed *et al.* [16] examined an innovative 1D reject band philter RBF array for the prevention of portable devices leaking around 2.45 GHz of radiation. The proposed RBF arrays are made from 8-unit FR-4 substrates mounted on one side. Across each cell adjacent to the unit is a separation of 2 mm. The basis of the individual cell unit design is a modified Minkowski configuration with fractal open-loop resonators. In combination with an open stop line, this increases the selection of a philter-stopping group response. The performance of the unit cells is evaluated and calculated numerically and analytically. The next step is to create and simulate an optimal RBF array to evaluate the 2.45 GHz (SAR) specific rate of absorption. The number of items studied in the SAR effect in the human thigh a very high decline of 0.912 to 0.352 W/kg. Finally, the field strength is measured and found just below the Wi-Fi antenna and reduced from 497.1 to 171 before and after the application of the project array beneath the personal laptops.

Kumar *et al.* [17] studied inside a numerical homo-genous human muscle phantom model; the specific

absorption rate (SAR) field of the inverted expected F antenna (PIFA) is examined. Two antennae; PIFA meander and PIFA wrinkle are inserted and resonated at 2,4 GHz simulated. The proposed design has a scale of 25 × 22.4 mm on Rogers RT/droid 5880 substrates, 20 miles thick. The architecture proposed claims ultra-wideband with a bandwidth of over 1.5 GHz. The meaning of various human tissue simulations is derived from the antenna up to 30 mm apart. At a distance of 1 mm to the antenna plane, the antenna's highest SAR value in human muscle tissue is 0.87 W/kg and 2.1 W/kg. The specification gives quite an increase of -21,57 dB and -22,3 dB inside the conducting tissue.

Jenshiya *et al.* [18] analyzed Assessment by an arrangement of the rectangular-shaped microstrip patch antenna of a particular absorbing rate of the human brain. An antenna is a transducer that transforms and transmits electronic signals into EM waves. The efficiency of an antenna is determined by its bandwidth, gain, loss of return, and so forth. Many types of antennas are available, but for many applications, microstrip patch antennas are widely used due to their low profile, lightness, low cost, versatility in the feeding system, reliability, manufacturing ease, etc. Despite the many benefits, it has significant disadvantages, including restricted bandwidth, low profits, and high return losses. FR-4 materials are used to deal with these commonly averaged inconveniences across the whole body (usually 1 gram or 10 grams of tissue) or over a limited amount of samples. The specific absorption rate (SAR) is a calculation of any amount of radiation absorbed into the electromagnetic field by the human body. It has a value of 1 watt/kilogram and is defined as the energy absorbed by weight. The average SAR of a body is usually 1 g or 10 g of tissue over a limited volume of sample. For the antenna proposed, the VSWR and return loss are measured to determine antenna efficiency, and a maximum gain of 4.43 dB at 10.8746 GHz is given by the proposed antenna. The antenna presented also measures a SAR value of the IEEE standard of 0.11109 W/Kg for 1 g of tissue. A microwave studio CST (Computer Simulation Technology) device was used to build the conceptual human head model and antenna.

Bhargava *et al.* [19] Unintentional over-exposure to non-standard cell phone radiation may be measured in certain situations. The vast limit of mobile telephone radiation interacts with the human body, which can affect human health. The scope of the physiological impact is anticipated in fragile organs or tissue such as the eyes, brain, skin, etc. with a small rise in temperatures. The subsequent thermo-physiological response of body tissues to the overwhelm limit of cell phone radiation is still not fully complied with. The purpose of this study is to examine the effects of cell phone over-exposure to the real absorption rate (SAR) and the rise in pressure in human 3D interconnected models. The analysis focuses on variations in electromagnetic (EM) absorption coefficient, with higher power levels between different use patterns. The effect of three different use patterns — voice calling, video calling, text-on SAR and distribution of temperature in various heads tissue types is systematically investigated. This paper also discusses the impacts of various consumer age SARs, radiated power, and gap distances of cell telephones and human heads on their temperature profiles. The findings from the study indicate a high impact of mobile exposure on the voice call location in light of safety guidelines. Analogies with an adult and a 7-year-old kid's head template are then measured for the voice calling position at various gap ranges. Moreover, the findings show that the head of the infant is often higher than the head of the adult cell phone radiation. The absorption rate in the tissue improves as the distance between your cell phone and head increases and the radiated power depends on your dielectric and temporal tendency. The findings would help to describe the exposure levels to the power of the mobile telephone and the gap between the user of the mobile phone and thermally-physiological aspects.

Ali *et al.* [20] this paper to design a new PIFA for apps for low-SAR mobile phones. The designed PIFA antenna comprises the upholstery of FR-4, the shortening wall and the base of F R-4, and a thrilling (feeding port) of the second content layer on the top of the first material layer. SAM head and hand imagination are to be used as a consumer's head and hand. In this model, the time-domain solver uses an adaptive meshing method for the hexahedral mesh. The result was obtained using MWS CST software based on the final adaptable working. With ZVA 67 vector analyzer, measurement results are obtained. The simulated findings and the investigations are roughly similar. The antenna has a high gain for both frequency bands (900 MHZ and 1800 MHZ) at a radiation efficiency of about 90 percent. Furthermore, the proposed SAR analysis of the antenna demonstrates low SAR capabilities for human use which compete with safe SAR specifications.

The electromagnetic wave (EM) is experienced by the human body from the aforementioned discussions, and some unintended effects arise in the tissue [15]. A major design problem to minimize SAR value in various simulated human tissue from the antenna up to 30 mm is the contamination leakage from portable systems of about

2, 4564 GHz [16, 17]. The rate of tissue absorption rises with a decrease in the gap between the cell phone, and the head, including restricted bandwidth, low gain, and high return losses [18, 19]. The rate of tissue absorption is increasing. Radiation is strong in the SAR study of the proposed antenna. This new work explores the design of the SAR reduction technology for a diverse layer of the human head model and the SAR restriction SAR ferrite sheet connection design review.

3. Amended Planar Inverted F- Antenna (PIFA) With Ferrite Sheet Attachment

Antennas are a link in a communication system between the transmitter and the free space or the free space and the receiver. The antenna will become an important part of the system as communication devices become small. New trends in antenna design focus primarily on antenna compactness, robustness, and compatibility with existing RF circuit components. The use of mobile phones and wireless communication technology has increased exponentially. In today's world, everybody uses mobile phones that use EM waves to penetrate human tissue. Human tissues are impaired by the absorption of these EM waves. It is, therefore, necessary to reduce the impact of electromagnetic energy on the human head when using a mobile phone. Measuring the absorption of EM waves by human tissue is known as the Specific Absorption Rate (SAR). Concerns regarding safety aspects and the dangerous effects of EM waves are therefore required. The antennas work with most cellular uses the global system for mobile devices (GSM)-865/900, remote cellular (DCS)-1900, PCS-1950, universal mobile transmission (UMTS)-2200, and long-term development bands (LTE). They are used for mobile device applications. Wireless antennas are also provided. The antennas suggested have a narrow bandwidth SAR size in all frequencies. Existing work faces many problems such as high radiation pattern; increase operating frequency, and Specific Absorption Rate is high and more expensive. The main challenge in the Planar Inverted F-antenna and Simulated Magnetic rod is Narrow bandwidth and Low reliability. Similarly, the Monopole and Planar Monopole antennas are used in existing techniques to reduce the SAR value. Monopole and Planar Monopoles are high radiation patterns with a metal strip and a high operating frequency.

Fig. 1. (Color online) Amended Planar Inverted F- Antenna (PIFA) With Ferrite Sheet for SAR Reduction.

Figure 1 shows the amended Planner Inverted F-Antenna (PIFA) with ferrite sheet for SAR reduction. In this proposed Design, a Simulated Magnetic rod is designed and simulated with a Planar Inverted F- Antenna (PIFA). A simulated Magnetic rod (SMR) is a type of implemented meta-material in several antennae and it is also used to reduce SAR Value. The main challenge in the Planar Inverted F-antenna and Simulated Magnetic rod is Narrow bandwidth and Low reliability. Consequently, implementing the Radiating Blotch within the antenna improves bandwidth and Reliability. Inside the Antenna Design Ferrite sheet attachment for SAR reduction. The Ferrite Sheet Crafted from ultra-thin mixtures, our ferrites have a sized, lightweight then low-cost component, of iron, nickel, and zinc oxides. They reduce EMI better while being open to the regular control system. Using the Ferrite Sheet Attachment in the antenna achieves High reliability and reduces the Specific Absorption Rate. Existing Meta-material is used for SAR reduction, but it works for a limited range of wavelengths and is difficult to manufacture. Finally, Radiating Blotch and Simulated Magnetic Rods are used in an Amended Planar Inverted F-Antenna; it operates at low operating frequencies. After this antenna design, the Evaluation of SAR is simulated in the 3D radiation pattern of the antenna with and without the Ferrite sheet and the radiation toward the human head is condensed by retaining a Ferrite sheet among the mobile as well as the head model, in this case, the distance between the phone and the Ferrite Sheet is 10mm. The head model is simulated using the HFSS with the planar inverted F-Antenna design stated below.

3.1. Planar Inverted F-Antenna (PIFA)

The PIFA antenna consists of a ground plane, a radiation component, a power supply cable, and a wire or strip connected between both the ground plane and the top platform. The regular configuration of the PIFA is shown in Fig. 2. It consists of a grounded monopole antenna that runs parallel to a ground plane. The antenna

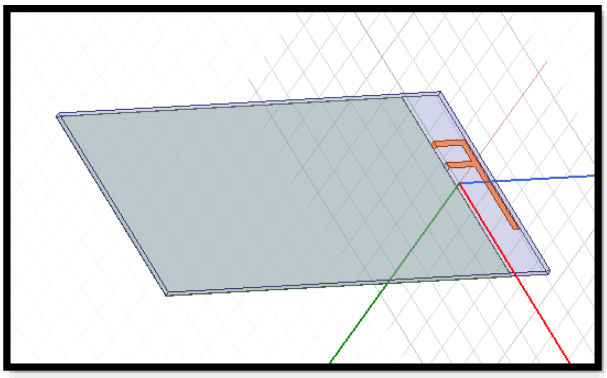

Fig. 2. (Color online) Structure of Planar Inverted F- Antenna Design.

is fed from a point that is situated between the grounded end and the antenna. At the bottom at the point where the wire falls to the ground plane, a feed wire feeds the antenna. The PIFA is an attractive wireless antenna for systems with very small wireless antenna space. Adding a short circuit strip allows good measurement of the output current with a top plate.

The top plate's height, width, and the feed wire's position are the model variables for this antenna. The PIFA feeding cable is a semi-rigid coaxial with a central leader extending past the end of the exterior conductor. The stage revealed a small hole in the ground floor at the bottom; the coaxial external conductor is plugged. A good way to reduce the antenna size is the standard PIFA-type short circuit board, which results in a small impedance bandwidth.

The estimated resonant rate of Amended PIFA is:

$$X1 + X2 = \sigma/4 \quad (1)$$

$$\text{While } W/X1 = 1,\ X1 + H = \sigma/4 \quad (2)$$

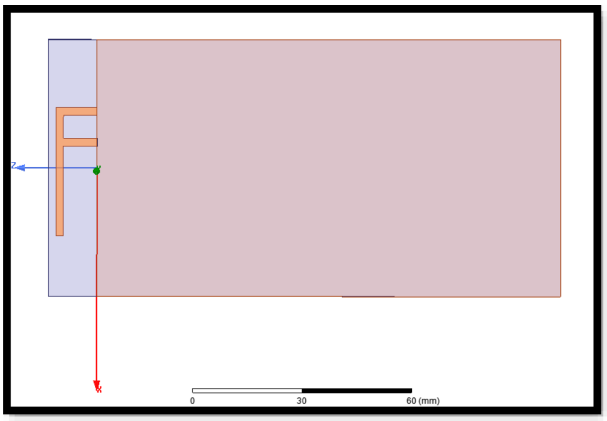

Fig. 3. (Color online) Top View of Amended PIFA Antenna.

$$\text{While } W=0,\ X1 + X2 + H = \sigma/4 \quad (3)$$

Where the PIFA duration is X1, X2 and the PIFA W width decreases, the resonant frequency also decreases. The micro-band antennas are typically half-wavelength, whereas the fourth wavelength of the PIFA antenna. Consequently, it is ideal for medical use. Impedance match is achieved by increasing the distance between the feed and short pins. For good matching of impedance, the shorting pin and single feeding are within the slot. The antenna array of this antenna depends on the location of the radiated power in space. Radiation properties, i.e. field power, flow density, polarization then phase, stand as follows. Contrary to the impedance bandwidth of the antenna, the supremacy factor R is reciprocal.

$$R = \text{Energy Kept / Control Lost} \quad (4)$$

Between the open end as well as the short edge, the feed will be located. The input impedance is regulated by the feed target. The shorting ring is generated by a plate in the Top View of Amended PIFA is shown in Fig. 3. By maximizing the feed widths and shortening the plates, it is possible to generate PIFA with a substantially wider bandwidth than has previously been reported. The length here is X1, the width is X2. The feeding is situated at a distance from D as well as from the air at height H. A dielectric with δr permittivity is the layer. To evaluate the impedance, the distance between both the feeding and the small pin is modified. Dependent on W, the frequency response varies. The entire patch width is the same as the short stick while W = X2. A simulated magnetic rod with Planar Inverted F-Antenna (PIFA) is designed and simulated in this proposed design. A simulated Magnetic rod (SMR) is a type of instigated meta-material in numerous antennae then is similarly used to decrease SAR Value.

3.2. Simulated Magnetic Rod

Simulated Magnetic Rod (SMR) seems to be a type of Meta material used for antennas and microwaves throughout multiple development applications. Using the unique characteristics of Meta-materials that do not exist naturally will improve the efficiency of various microwave instruments. The specific absorption rate (SAR) is assumed to precede these various mobile bands. The architecture of the SMR is focused on a dielectric film with metal strips on the bottom surface. The scientific viewpoint addresses the conceptual dimensions, procedures for simulation development, and the setup of measurements used to define the unit cell of the SMR.

3.2.1. Design of Simulated Magnetic Rod Structure:

We designed and applied a capacitive SMR grating device in addition to the SAR values. The conductivity film is used with the printed images on the top and bottom of the dielectric metal strips. When the incident plane wave is parallel to the configuration of the SMR, the impedance (P) during the first and second conductive layers can be expressed as (5). Between the second conducting layer and the conductive soil surface, impedance (P11) may be expressed as a (6). The complete impedance can therefore be obtained (P_{22}) Following (7)

$$P = \frac{-jd\lambda}{\pi\varepsilon(b-2a)b} \tag{5}$$

$$P_{11} = jkE \qquad (B\sqrt{\beta_1}\ E \le 1) \tag{6}$$

$$P_{22} = \frac{P_{11}P}{P_{11}+P'} \tag{7}$$

Here β as well as β_1 are the permittivity of the material placed in the gratings as the layer between the mesospheric range pair and the ground plane. P_{22} requires an infinite value when ordered to control a high-impedance surface (HIS), apart from the P_{22} denominator, it must remain zero. The frequency of operation for HIS may therefore be defined

$$\text{Freq}_{\text{HIS}} = \frac{t}{\pi\sqrt{2\sqrt{\beta E b(b-2a)/d'}}} \tag{8}$$

Where t is the velocity of light and the measurements of the deliberate SMR assembly are as charts: β = 5.4, β_1 = 2, *a* = 0.3 mm, *b* = 4.5 mm, *d* = 0.4 mm, and E = 5 mm. From (8), we can imagine that 1946 MHz was the exploratory core frequency at the high impedance surface (Freq_{HIS}). We can also measure the process of reflection of the designed SMR structure using the full-wave simulator (ANSYS HFSS). Besides slave boundary conditions, we must create an immeasurable periodic structure by the master and then a normally incident plane wave by Ex polarization. For the reflection process, the SMR range is typically demarcated from -80 to 95 and then simulated after 1790 MHz to 2280 MHz. In addition to periodicity (b), Freq_{HIS} can remain regulated by parameters of the SMR structure, such as the height of the lower substrate (E), and the eighth of the upper substratum (2d). Among the constraints, the height of the upper substrate (2d) and the height of the lower substrate (E) remain the leading factors. The height of the upper substratum (2d) and the lower substratum (E) decreases as well as increases along with Freq_{HIS} may remain downshifted individually. We need a finite capacitive grating SMR structure to be used in mobile receivers by way of the capacitive grating SMR structure by double layers in the figure and it remains a model of an immeasurable structure. The metalized side of the finite SMR assembly is connected to the mainboard to avoid wave penetration to the side path.

To improve the performance and bandwidth of PIFA at low frequencies, the ground plane under the framework of the SMR should also be removed by 2, 5 mm. The total size of the antenna, along with the SMR structure, is 65 mm (length) approx. 20 mm (width) approx. 5 mm (height). If the size of the SMR range increases, the SAR is reduced even further, but the antenna's output in a low band is reduced. The width of the SMR framework and that of the non-SMR framework were planned to be 7.5 mm and 4.5 mm respectively, after initialization. The PIFA and the touch-sensitive grating SMR system examine higher and lower bands and only high bands in this layout. This is because the mobile terminal does not have enough antenna space to design an SMR structure that can be worked on both low and high bands. However, need a novel approach using an integrated PIFA and SMR scheme. In the SMR and PIFA systems, the present distribution is high-banded in the same direction. This allows the PIFA to be positioned near the SMR system in contrast to an ordinary metal surface. At the same time as grounded SMR structural parameters, PIFA measurements were calculated. For the pentaband to satisfy unique and multi-impedance conditions (924 Alto 1060 MHz and 1810 Alto 2190 MHz), we have optimized the longitude and shape of the PIFA on the SMR structure. The design length of the antenna for the low and high bands is 60 mm and 40 mm. The integrated antenna is compared to the traditional PIFA without an SMR structure with the properties of a pentaband with greater efficiency and lower SAR values. Limited bandwidth and poor reliability are the major challenges in the Planar Inverted F antenna and virtual magnetic rod. But to maximize bandwidth and reliability we have incorporated radiating blots within the antenna.

3.3. Radiating Blotch

Proper slots are inserted in the radiating blotch to gain multiple band activity. And to maximize the bandwidth, proper slots are added on the ground of the Planer Inverted F-Antenna. Over the radiating blotch, the slots are built. Three slots are Slot 1, Slot 2, and Slot 3 in the PIFA Antenna. Slots 1 and 2 are 0.21 cm × 1.14 cm in the same size. Slot 3 has a size of 0.21 cm × 62 mils. These

slots are used in the antenna to excite multiple resonances. The Planar Inverted-F Antenna is 62 mil from the ground plane.

PIFA consists mainly of mounting a shortened radiating strip or blotch over the mobile phone's system ground plane. This form of antenna reveals a structure in three dimensions (3-D). The basic or lowest frequency resonant modes of the antenna are usually operated in their resonant modes of quarter-wavelength. The PIFA consists of a ground plane, a top blotch, a feed tube, and a short-circuit loop for the top blotch to the ground plane.

The short strip or pin results in such a quarter-wave resonator, or even several resonant modes, based on the blotch structure. Because of this, the blotch length is decreased by at least 50 % relative to the traditional half-wave blotch. It is possible to configure PIFAs to work over multiple frequencies by splitting the short-circuited blotch with slots. The PIFA bandwidth can also be modified by improving the ground plane dimensions, for example by reducing the ground plane dimensions, the antenna bandwidth can be increased effectively. The radiating blotch is designed for lightweight handset applications with a total volume of 7.1 m × 14.2 cm × 62 mil. The antenna is mounted on a ground plane of 7.1 cm × 12.85 cm, which in realistic mobile phones is considered to be the width of the PCB panel. The PIFA is printed on a 62 mil height ADK sub strum and the 0.0009 dielectric constants are used. The PIFA is developed with Relative Permittivity and Permeability as 2.2 and 1 along with the Lande G factor 2. Slots were produced to excite numerous resonances in the antenna on the radiating blotch structure. Radiating Blotch improves narrow bandwidth and performance and then implemented a Ferrite Sheet Attachment for SAR reduction.

3.4. Ferrite Sheet Attachment

The ferrite sheet is placed between the antenna and the human head and improves SAR production. The GSM 900 for research was used to reduce the SAR antenna. The FDTD process, combined with a detailed human head model, is often used to study various positions, measurements, and particular ferrite sheet materials. SAR performance reduction performance during simulations, the ferrite layer is accurately represented by dispersive models of all dielectrics. In addition, the SAR has simulated the performance capacity of the cell phone model must be set. The ferrite sheet has a total volume of 71 × 142 mm × 0.01 mm. The pad is connected to the PIFA sub-storm. The ferrite sheet is printed with a relative permeability of 13 and 1010. The efficiency of the reduction of SAR relies on its height and width. The disparity between the mobile person and head models is diverse and SAR output increases afterward. This is because there are also some constant dielectric losses, conductivity, density, and electromagnetic tangent. The ferrite sheet between both the mobile models and the head model can be decreased by 20 mm by the distance. For the 1 gm and 10 gm average SAR, the value of the ferrite sheet attachment has been decreased. The result implies that the only approach to increasing the SAR spatial limit is to suppress the total current on the front side of the conduction box. This is because the reduced power intake in the brain is considerably greater than the energy consumed in the ferrite sheet.

4. Results and Discussions

The proposed methodology is implemented in ANSYS HFSS and the simulation results are discussed below. The proposed methodology is stated in section 3 above and the detailed description. The proposed approach is implemented with the following device specification on the working framework of ANSYS HFSS.

Platform : ANSYS HFSS
OS : Windows 10
Processor : Intel core i5
RAM : 12 GB RAM

4.1. Simulation Outputs

The Ferrite Sheet with Amended PIFA for SAR Reduction simulation outputs are shown below figures and also the simulated representation of each parameter in the simulation has been deliberated following.

Figure 4 states the Return loss of the Planar Inverted F-Antenna of the proposed Ferrite Sheet attachment with Amended PIFA for SAR Reduction. The return loss of an antenna is a number that signifies the percentage of radio

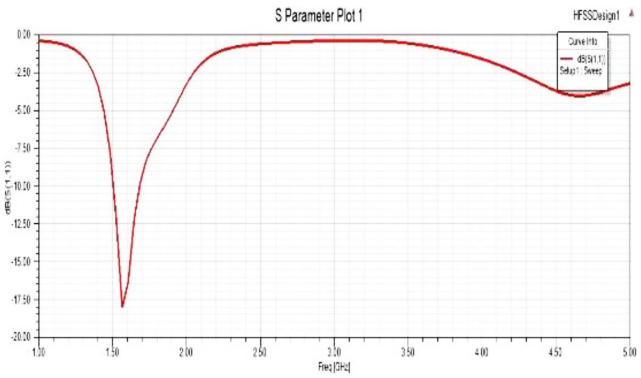

Fig. 4. (Color online) Return loss of Planar Inverted F-Antenna.

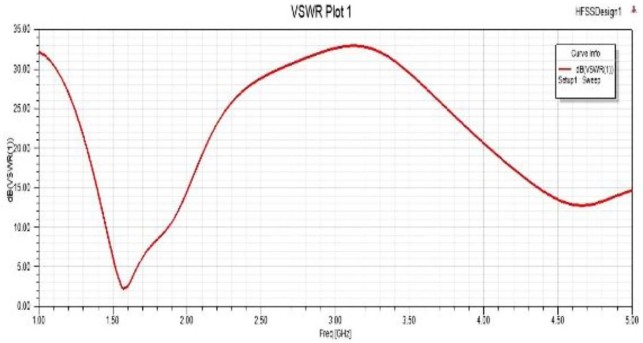

Fig. 5. (Color online) VSWR of Planar Inverted F- Antenna.

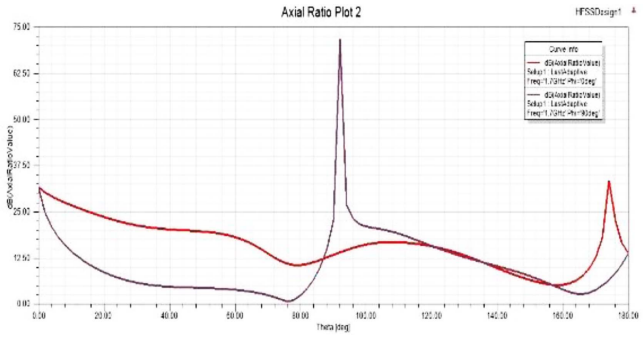

Fig. 6. (Color online) Axial Ratio of Planar Inverted F-Antenna.

waves that arrive at the antenna input that is rejected in comparison to those that are accepted. It is specified as a short circuit in decibels (dB).

Figure 5 shows the Voltage Standing Wave Ratio (VSWR) of the Planar Inverted F- Antenna of the proposed Ferrite Sheet attachment with Amended PIFA for SAR Reduction. For antennas, the VSWR is always a precise and positive value. More power is transmitted to the antenna and the antenna is better suited to the transmission line when the VSWR is reduced.

Figure 6 states the axial ratio of the Planar Inverted F-Antenna of the proposed Ferrite Sheet attachment with Amended PIFA for SAR Reduction. In this axial ratio of PIFA, the proportion of a circularly polarized antenna pattern is major to minor axes. This ratio would be 1 (0 dB) if an antenna had perfect circular polarization. The axial ratio of the antenna can be calculated using the polarization efficiency equations by monitoring the received signals of the circularly polarized antenna at two distinct axial angles when the auxiliary antenna operates in the left- or right-hand modes.

Figure 7 states the Group Delay of the Planar Inverted F- Antenna of the proposed Ferrite Sheet attachment with Amended PIFA for SAR Reduction. Group delay in signal processing refers to the delays that occur as a

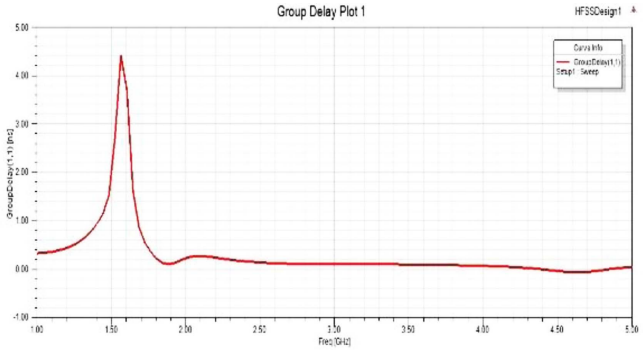

Fig. 7. (Color online) Group Delay of Planar Inverted F-Antenna.

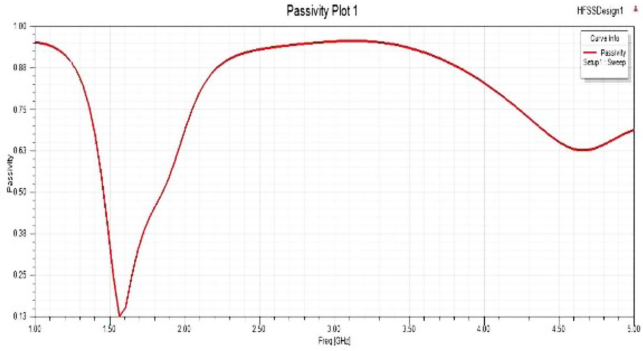

Fig. 8. (Color online) Passivity of Planar Inverted F- Antenna.

signal passes through a linear time-invariant system (LTI). As a result, the waveform of the signal is distorted as it moves through the system.

Figure 8 states the passivity of the Planar Inverted F-Antenna of the proposed Ferrite Sheet attachment with Amended PIFA for SAR Reduction. The proposed model's passivity of PIFA reaches 0.95 at 1 Hz frequency

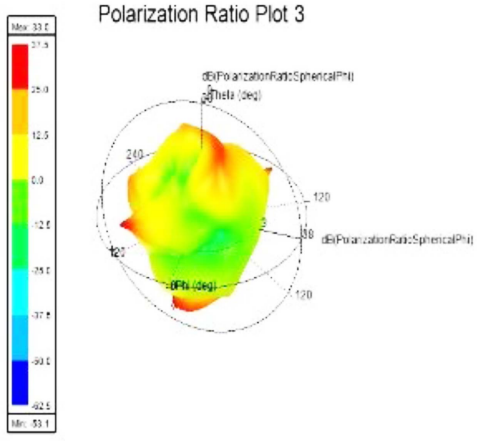

Fig. 9. (Color online) Polarization ratio of Planar Inverted F-Antenna.

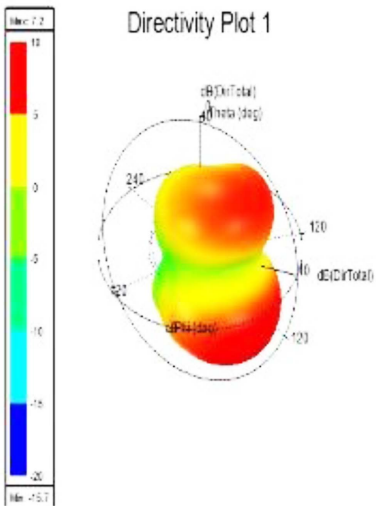

Fig. 10. (Color online) Directivity of Planar Inverted F-Antenna.

and reaches 0.72 at 5 Hz. Similar to this, passivity moves in waves as the frequency rises.

Figure 9 states the polarization ratio of the Planar Inverted F- Antenna of the proposed Ferrite Sheet attachment with Amended PIFA for SAR Reduction. The signal is constrained in a main linear polarization mode and is measured by the polarization ratio. After propagating through a device or system, it is defined as the ratio of power in the primary polarization mode to power in the orthogonal polarization mode, expressed in decibels (dB).

Figure 10 shows the Directivity of the Planar Inverted F- Antenna of the proposed Ferrite Sheet attachment with Amended PIFA for SAR Reduction. The directivity of the antenna to the desired direction or to enhance the

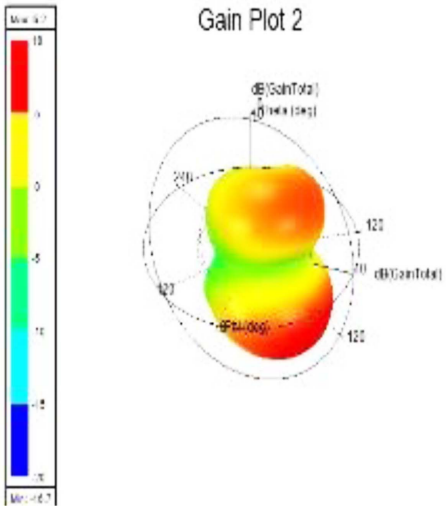

Fig. 11. (Color online) Gain of Planar Inverted F- Antenna.

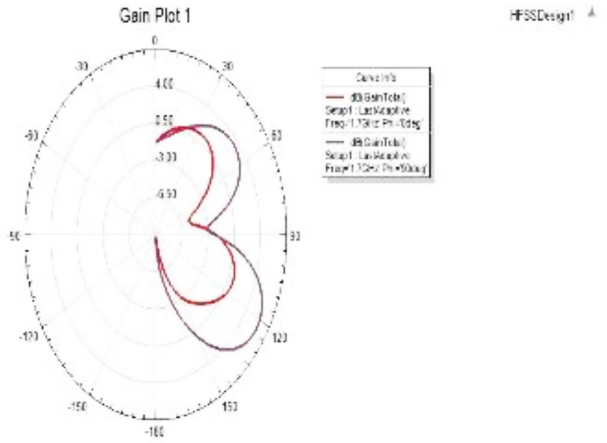

Fig. 12. (Color online) Radiation Pattern of Planar Inverted F-Antenna.

operating bandwidth and reliability in a Plannar Inverted F-Antenna.

The ability of an antenna to emit more or less in any direction as compared to a theoretical antenna is known as antenna gain. Figure 11 states the Gain of the Planar Inverted F- Antenna of the proposed Ferrite Sheet attachment with Amended PIFA for SAR Reduction. An antenna would radiate evenly in all directions if it could be constructed as a perfect sphere.

Figure 12 states the Radiation Pattern of the Planar Inverted F- Antenna of the proposed Ferrite Sheet attachment with Amended PIFA for SAR Reduction. A radiation pattern of Planner Inverted F-Antenna's signal as a function of the direction it is facing away from the

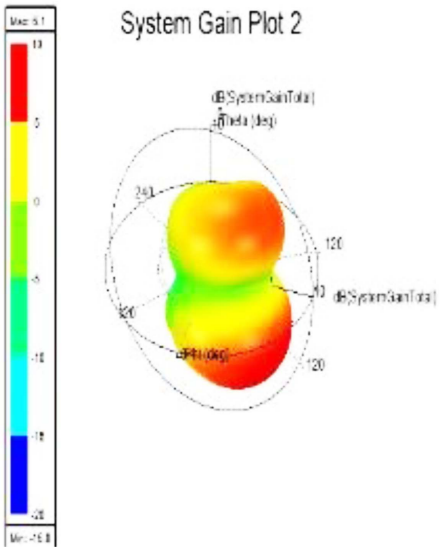

Fig. 13. (Color online) System gain of Planar Inverted F-Antenna.

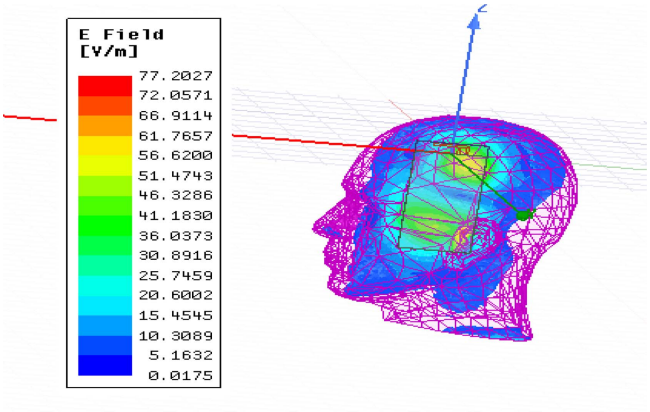

Fig. 14. (Color online) Electric Field of Planar Inverted F-Antenna.

antenna. The furthest range of the antenna exhibits this signal variation as a function of the arrival direction.

Figure 13 shows the System Gain of the Planar Inverted F- Antenna of the proposed Ferrite Sheet attachment with Amended PIFA for SAR Reduction. The system gain of the antenna has no units. In the perfect scenario, where all of the signal given by the transmitter was contained within the ideal beam shape and none of it was lost, it would be at its highest potential value. In reality, this ideal cannot be realized since the signal cannot be condensed into an ideal signal form and some of the transmitter power must be lost to overcome electrical resistance in the antenna.

Figure 14 states the Electric Field of the Planar Inverted F- Antenna of the proposed Ferrite Sheet attachment with Amended PIFA for SAR Reduction. A stronger E-field incident upon an antenna will result in a greater voltage

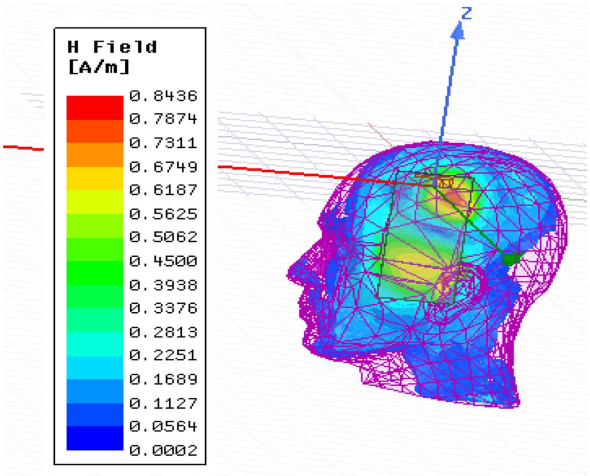

Fig. 15. (Color online) Magnetic Field of Planar Inverted F-Antenna.

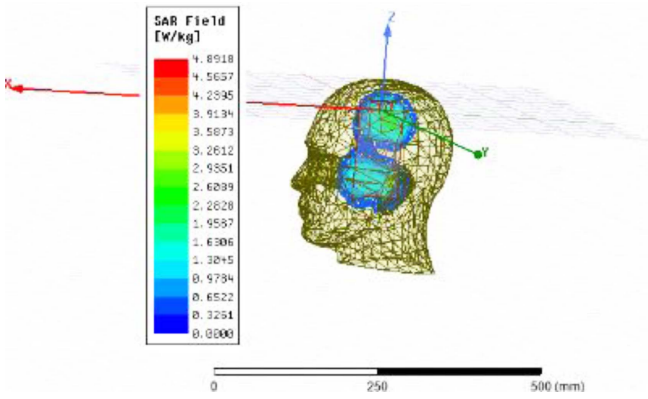

Fig. 16. (Color online) SAR Reduction of Planar Inverted F-Antenna.

difference between the antenna's terminals. The electric field and voltage are also related to SAR reduction.

Figure 15 shows the Magnetic Field of the Planar Inverted F- Antenna of the proposed Ferrite Sheet attachment with Amended PIFA for SAR Reduction. The magnetic field (H-field) coming from the EUT is measured using the magnetic loop antenna. When the signal is tested lower frequency point is mandated by the product standard, and measurement of the H-field is frequently specified.

Figure 16 states the SAR Reduction of the Planar Inverted F- Antenna of the proposed Ferrite Sheet attachment with Amended PIFA for SAR Reduction. The PIFA has strong SAR characteristics and is resonant at a signal. This looks like an inverted F. Popularity of the Planar Inverted-F Antenna is due to its low profile and omnidirectional layout for the reduction of SAR.

4.2. Comparison Stratagems

To determine the complete contrast either with or without ferrite sheet attachment of the proposed PIFA antenna, the following are:

Table 1 states the comparison of with and without ferrite sheet attachment for Planar Inverted F-antenna based with and without ferrite sheet Attachment based on SAR reduction against Bandwidth, Gain, system gain, and

Table 1. Evaluation of PIFA Antenna with as well as without Ferrite Sheet Attachment.

Parameters	Without Ferrite Sheet	With Ferrite Sheet
SAR	0.3918 W/Kg	0.3261 W/Kg
Bandwidth	0.1844 GHz	0.198 GHz
Gain	6.7 dB	6.2dB
System Gain	5.5 dB	6.1dB
Directivity	7.0 dB	7.2 dB

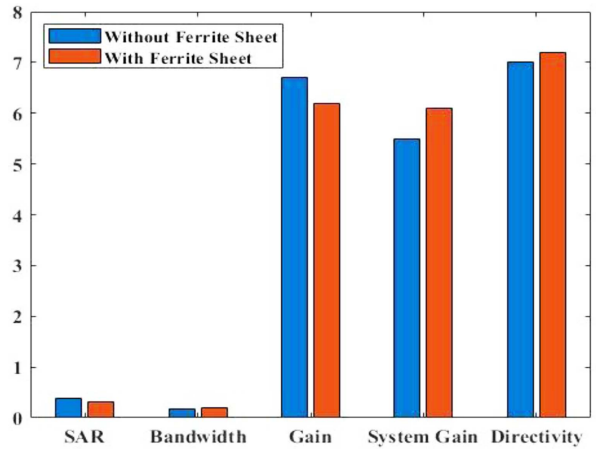

Fig. 17. (Color online) Overall Comparison for Performance metrics in proposed PIFA Antenna.

Directivity. Some characteristics reach their maximum value when compared with as well as without the ferrite sheet. With the ferrite sheet, SAR and gain are at their highest values. Additionally, without a ferrite sheet, the value of bandwidth, system gain, and directivity are at their lowest.

Figure 17 shows the Overall Comparison of Performance metrics in the proposed PIFA Antenna. SAR, Bandwidth, gain, system gain, and directivity are compared for both with and without a sheet of ferrite SAR-based attachment. In terms of bandwidth, system gain, and directivity, the value with a ferrite sheet is higher than without a ferrite sheet. Additionally, the value of SAR and Gain with a ferrite sheet is lower than without a ferrite sheet.

5. Conclusion

The antenna is becoming an important part of the system as the communication devices get smaller. In this document, a modified Planar Inverted F-Antenna (PIFA) is designed and simulated. At a distance from the grounded end, the antenna is fed from the midpoint. The antenna design is smaller and more portable, and without the need for foreign matching parts, the designer can control the corresponding impedance. A simulated magnetic rod (SMR) is a meta-material type used in multiple antennas and is also used to reduce the SAR value. Narrow bandwidth and poor reliability are the main challenges for the Planar Inverted F-antenna and Simulated Magnetic Rod. The Evaluation of the head model is simulated using the ANSYS HFSS and this organization results in with and without ferrite sheet Attachment based on Specific Absorption Rate (SAR) is 0.3261 W/kg.

References

[1] A. Nada, W. S. El-Deeb, and A. Zaghloul, Curr. J. Appl. **20**, 1 (2017).
[2] Z. M. Lwin and M. Yokota, Intrn. Conc. on Big Data Analysis and DL Appl. (2018) pp 191-198.
[3] B. Lakbir, F. Riouch, A. Tribak, J. Terhzaz, and A. Bouyahyaoui, Angel Mediavilla Sanchez. In 2018 6th ACM Trans. Multimedia Comput. Commun. Appl. (ICMCS) (2018) pp 1-6.
[4] A. Kamalaveni, M. Ganesh Madhan, AEU - Int. J. Electron. Commun. **70**, 1192 (2016).
[5] Z. M. Lwin and M. Yokota, In 2018 IEEE 7th Global Conference on Consumer Electronics (GCCE) (2018) pp 1-2.
[6] R. Boopathi and S. K. Pandey, In 2015 13th IEEE Electromagn. Compat. Mag. (2015) pp 176-178.
[7] V. Stanković, D. Jovanović, D. Krstić, and Nenad Cvetković, In 2015 9th International Symposium on Advanced Topics in Electrical Engineering (ATEE) (2015) pp 392-397.
[8] M. F. Ali, Indian Journal of Radio & Space Physics (IJRSP) **43**, 235 (2017).
[9] S. Bhattacharjee, M. Monojit, and S. R. Bhadra Chaudhuri, Progress In Electromagnetics Research **55**, 143 (2017).
[10] M. I. Hossain, M. R. I. Faruque, and M. T. Islam, Hand. **36**, 1 (2015).
[11] D. Mitra, D. Soumyadeep, and P. Shubhadip, In 2019 Int. J. Antennas Propag. (2019) pp 1-4.
[12] T. Alam, R. I. F. Mohammad, and T. I. Mohammad, Appl. Phy. A. **122**, 170 (2016).
[13] S. Imaculate Rosaline and Singaravelu Raghavan, J. Electromagn. Waves Appl. **29**, 2330 (2015).
[14] E. K. Hur, J. S. Jung, S. A. Cho, and S. W. Choi, U.S. Patent. 9,847,577 19 (2017).
[15] Z. M. Lwin and M. Yokota, AEU - Int. J. Electron. Commun. **104**, 91-98.
[16] Ahmed, S. Hayder, and A. Taha Elwi, Int. J. Electron. **7**, 236-248.
[17] R. Kumar, L. S. Solanki, and S. Surinder, In 2019 6th Int. J. Signal Process. (2019) pp 755-759.
[18] P. R. Jenshiya, K. Madhan Kumar, and H. Riyaz Fathima, ICTACT Journal on Communication Technology **10**, 1923 (2019).
[19] D. Bhargava, N. Leeprechanon, P. Rattanadecho, and T. Wessapan, Int. J. Heat Mass Transf. **130**, 1178 (2019).
[20] R. Ali, M. I. Ahmed, S. W. El-Deeb, and A. A. Shaalan, Curr. J. Appl. of Sci. Tech. **36**, 1 (2019).